ACS APPLIED MATERIALS & INTERFACES

Research Article

www.acsami.org

A Biodegradable Gel Electrolyte for Use in High-Performance Flexible Supercapacitors

Won Gyun Moon,[†] Gil-Pyo Kim,[†] Minzae Lee, Hyeon Don Song, and Jongheop Yi*

World Class University Program of Chemical Convergence for Energy & Environment, Institute of Chemical Processes, School of Chemical and Biological Engineering, Seoul National University, Seoul 151-742, Republic of Korea

Supporting Information

ABSTRACT: Despite the significant advances in solid polymer electrolytes used for supercapacitors, intractable problems including poor ionic conductivity and low electrochemical performance limit the practical applications. Herein, we report a facile approach to synthesize a NaCl−agarose gel electrolyte for use in flexible supercapacitors. The as-prepared agarose hydrogel consists of a three-dimensional chemically interconnected agarose backbone and oriented interparticular submicropores filled with water. The interconnected agarose matrix acts as a framework that provides mechanical stability to the gel electrolyte and hierarchical porous networks for optimized ion transport. The developed pores with the water filler provide an efficient ionic pathway to the storage sites of electrode. With these properties, the gel electrolyte enables the supercapacitor to have a high specific capacitance of 286.9 F g^{-1} and a high rate capability that is 80% of specific capacitance obtained in the case of a liquid electrolyte at 100 mV s^{-1}. In addition, attributed to the simple procedure and its components, the gel electrolyte is highly scalable, cost-effective, safe, and nontoxic. Thus, the developed gel electrolyte has the potential for use in various energy storage and delivery systems.

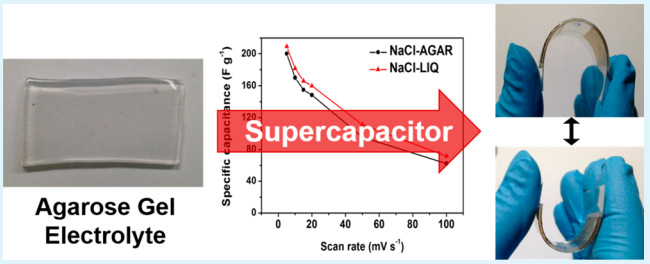

KEYWORDS: *electrochemistry, supercapacitor, gel electrolyte, agarose hydrogel*

1. INTRODUCTION

As one of the consequences of the global warming and energy crisis, the appetite for enhanced energy storage devices (ESDs) with higher energy and power densities has been increased considerably. Among the various forms of ESDs, supercapacitors are highlighted by virtue of their outstanding features that include a fast charge−discharge rate, long cycle life, and environmentally friendly nature.[1−3] Traditional supercapacitors use liquid electrolytes such as acid or alkali solution, similar to batteries.[4,5] However, this configuration impedes further applications for two reasons: The use of solutions makes the supercapacitor heavier, which causes difficulties in their integration, and the possibility of harmful electrolyte leakage requires that they be safely encapsulated, giving rise to increased costs.[4,6] Thus, solid polymer electrolytes (SPEs) have been developed as substitutes for a liquid electrolyte.

Supercapacitors based on SPEs are being considered as potential candidates to meet the expanding demand for portable, flexible ESDs. SPE-based configuration ensures that a supercapacitor would store and supply electrical energy and have a capacity sufficient to accommodate certain levels of transformation.[5] Typical SPEs are formed by direct dissolving salts such as $LiCF_3SO_3$, $LiN(SO_2CF_3)_2$, $LIPF_6$, $LiBF_4$, and $LiClO_4$, into an ion-coordinating polymer such as polyethylene-oxide (PEO), polyethylene-glycol (PEG), siloxane, and copolymers derived from them.[7,8] Such systems have been widely studied, and can be prepared by solvent casting, extrusion, hot pressing, lamination, or even by in situ polymerization.[8] However, the low electrochemical performance of this electrolyte configuration hampers their widespread use in various applications. This limitation, which stems from the relatively low ionic conductivity at room temperature ($10^{-8} < \sigma < 10^{-3}$ S cm^{-1}),[9,10] induces increased internal resistance and reduced charge storage properties, compared to an analogous liquid electrolyte configuration.[4] Tailored designing of the solid electrolyte plays a key role in determining the overall electrochemical performance of ESDs. It is generally accepted that high electrochemical performance can be generated with the properly formed electrode−electrolyte interfaces. The optimal physical-chemical properties of solid electrolyte, particularly its surface, can improve the ionic transport ability and is of both scientific and practical significance. Ion gels of polymeric networks that are swollen with an ionic liquid,[11,12] represent ideal candidates for integrating the key benefits of liquid and solid polymer electrolytes. The cohesive features of solid systems with liquid-like transport properties, would provide a plausible configuration because of their advantages including a high degree of flexibility, semisolid characteristics as well as high

Received: October 14, 2014
Accepted: January 26, 2015
Published: January 26, 2015

DOI: 10.1021/am5070987
ACS Appl. Mater. Interfaces 2015, 7, 3503−3511

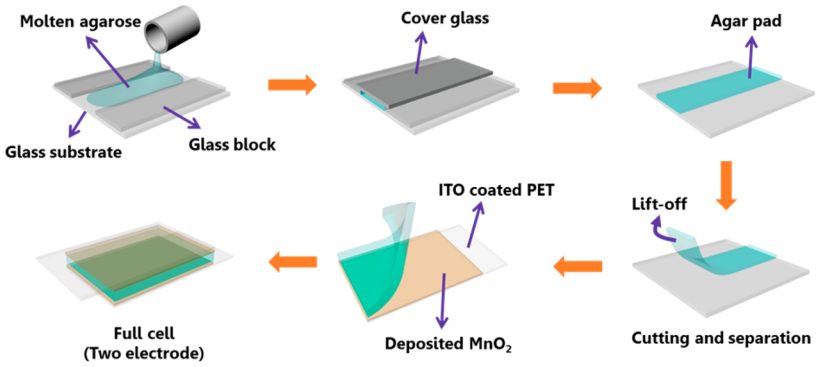

Figure 1. Schematic illustration showing the fabrication of an agarose-gel-mediated MnO_2 symmetric cell assembly.

ionic conductivity.[4,5,8] Conventional ion gel systems such as PVA−H_3PO_4, PVA−H_2SO_4, PVA−LiCl, PAN−PEG−$LiClO_4$, and P(VDF−HFP)−$EMIMBF_4$ have been reported.[9,13−16] These polymer-ionic liquid combinations show mechanical deformability and performance-oriented properties with a low probability of safety problems, owing to methods used in their fabrication.[12,13,17,18] However, the high cost of synthesis and environmental impact with toxicity concerns related to ion-gel chemicals are drawbacks for their reliable use.

An agarose-based hydrogel is a gelling constituent of agar with an agarobiose monomeric unit, which features submicrometer pores (pore sizes of 400−500 nm) and a high elasticity (Young's modulus of 116 kPa) and is both low in cost and environmentally benign.[19−23] The gelation of agarose involves the cross-linking self-assembly of molecules via hydrogen bonding[24] and results in the formation of a semiflexible water filled gel with a 3D porous structure.[25] Due to the high water content (>90% water) and interconnected pore structure, the agarose hydrogel is a soft, moldable and biocompatible medium with high ion mobility.[26] Furthermore, as a type of ion gel, the ionic properties of the agarose gels can be readily tuned by the incorporation of an ionic liquid as a functional filler that has negligible vapor pressure and is nonvolatile and flame retardant.

On the basis of the above-mentioned features, agarose-based hydrogels have been widely used in fields ranging from food production and biological research to various gel-based device systems such as ion current diodes, memristors, photovoltaic devices, and polyelectrolyte diodes.[26−32] To the best of our knowledge, however, practical applications of agarose gels as an electrolyte material in supercapacitor configurations have not been reported. Moreover, securing mechanical flexibility and environmental benignity of electrolytes while retaining their electrochemical performance continue to be a challenging issue.

Herein, we report a high-performance NaCl−agarose gel (NaCl−AGAR) for use in flexible supercapacitors by the direct incorporation of sodium and chloride ion pair into a hydrogen bonded cross-linking agarose gel. Through the self-assembly of agarose, which is stabilized by intra- and intermolecular hydrogen bonding, the three-dimensional (3D) porous structure of our gel enabled a high ratio of energy delivery with optimized ion transport channels. From a material design standpoint, the gel can be modified into various shapes and can be transferred to a conductive substrate, which is a scalable approach. In addition, due to the low unit cost for agarose gel and NaCl flakes, simple solution-mixing, heating, and casting methodology, these facile and cost-effective characteristics allow supercapacitors to be fabricated conveniently. In this respect, our tailored waterborne gel could be used as a conducting media in flexible devices owing not only to its simple production but also to its high capacitance that matches that of a liquid electrolyte configuration. Furthermore, the fact that NaCl and agarose are edible ensures the eco-friendly nature of our fabricated gel electrolyte. It is believed that NaCl−AGAR would provide a convenient and green route to incorporating a high-capacitance gel electrolyte in a supercapacitor, which permits such energy storage devices to be compatible for use in flexible electronics.

2. METHODS

2.1. Electrodeposition of MnO_2 Thin Film. An indium tin oxide-coated polyethylene terephthalate sheet (ITO−PET) was used as the substrate for working electrode. Prior to the deposition, the ITO−PET substrates (2 × 4 cm) were rinsed by ultrasonication in 1:1 mixture of iso-propanol and acetone. The electrodeposition was performed at room temperature using a WPG100 electrochemical workstation (WonATech) with a three-electrode system. A Pt plate and Ag/AgCl electrode were used as the counter electrode and reference electrode, respectively. $Mn(NO_3)_2$ (0.05 mol) and of $NaNO_3$ (0.075 mol) were dissolved in deionized (DI) water. The electrodeposition was performed potentiostatically at 1.0 V (vs Ag/AgCl) for various times (100, 200, and 300 s). After the electrodeposition, the as-synthesized films were rinsed with deionized (DI) water and dried at room temperature for 24 h.

2.2. Preparation of Gel Electrolyte Using an Agarose Gel. Various concentrations of NaCl solutions (0.1, 0.25, and 0.5 M, 100 mL) were prepared by combining a NaCl solution (5 M, Aldrich) and DI water followed by vigorous stirring. In sequence, powdered agarose (1 g, Sigma-Aldrich) was dissolved in the as-prepared solution (100 mL). The 1% (w/v) agarose solution was heated using a microwave oven. After the agarose had completely dissolved, the solution was casted onto a glass plate and allowed to gel on the plate at room temperature for 15 min. After cooling, the gel electrolyte derived from agarose gel was cut and separated (2 × 3 cm), and then assembled with MnO_2 electrodeposited ITO−PET electrode. The NaCl containing agarose gel is denoted as NaCl−AGAR. The NaCl aqueous solution is denoted as NaCl−LIQ. The electrochemical performance of NaCl−AGAR was compared with NaCl−LIQ.

2.3. Characterization. The morphology and composition of electrodepositied MnO_2 films were characterized by scanning electron microscopy (SEM, Carl Zeiss, SUPRA 55VP), X-ray photoelectron spectroscopy (XPS, Thermo, K-Alpha), and X-ray diffraction (XRD, Rigaku, D/max-2200). Electrochemical characterization was performed using an assembled full cell with the NaCl−AGAR with various NaCl concentrations (0.1, 0.25, and 0.5 M) under a two-electrode system. For the control group, 0.1 M NaCl−LIQ was applied as for the liquid electrolyte within a two-electrode configuration. Cyclic voltammetry (CV) and galvanostatic charge−discharge measurements were carried out using potentiostat (Iviumstat electrochemical analyzer, Ivium Technology) at potential window of 0−0.8 V

DOI: 10.1021/am5070987
ACS Appl. Mater. Interfaces 2015, 7, 3503−3511

and various current densities of 0.5−10 A g^{-1}, respectively. Electrochemical impedance spectroscopy (EIS) was investigated using potentiostat (Iviumstat electrochemical analyzer, Ivium Technology) at various applied potentials (0.4−1.6 V). The AC amplitude was 10 mV and frequencies of 0.01 Hz to 100 kHz were used. Three full cells (MnO_2/NaCl−AGAR/MnO_2) were assembled in series to drive red (1.2 V, 20 mA) light-emitting diode (LED) after charging each full cell for 30 s.

3. RESULTS AND DISCUSSION

The scheme for preparing the supercapacitor assembled with the NaCl−AGAR and two electrodeposited MnO_2 electrodes is illustrated in Figure 1. Details of the fabrication process are described in the experimental section. In this study, a MnO_2 electrode was introduced as a model electrode to evaluate the electrochemical properties of the assembled supercapacitor and the changes in the configuration of the gel and liquid electrolyte. Our strategy for fabricating NaCl−AGAR has several advantages, as follows: (1) The gel electrolyte is prepared through solution-mixing, heating and casting in ambient conditions; this process is facile, nontoxic, and cost competitive for use in preparing flexible supercapacitors. (2) The thickness of the gel is easily tunable by adjusting the number of the glass blocks used, as shown in Figure S1A (SI). In addition, the gel can be transferred onto any substrate such as glass, stainless steel, and plastic plates. It should be noted that the interfacial gelation method is industrially feasible because, with the help of the various casting frames, the size and shape of the gel electrolyte can be easily controlled, as shown in Figure S1B (SI). (3) The introduction of the polymeric current collector can provide flexible characteristics, which makes the gelation-based build-up a promising method for the further fabrication of larger flexible devices. As a result of these advantages, the use of an agarose gel as an electrolyte permits a flexible supercapacitor to be produced with ease by simply tailoring its physical requirements.

The synthesized NaCl−AGAR is transparent and thin, as shown in Figure 2A, which makes it suitable for exhibiting bendable and flexible characteristics. Cross-sectional SEM images of this gel, obtained after the freeze-drying process, verifies that the gel is interconnected in a 3D manner with an open porous structure, as shown in Figure 2B. The pore size of the gel approximates a submicrometer scale, as previously reported.[33,34] The smaller pore size and volume compared to those of the gel itself is due to the sublimated volume of the water molecules, which were trapped in the inner pores before the freeze-drying process.[35] A supercapacitor assembled with the NaCl−AGAR and two MnO_2 electrodes are shown in Figure 2C. The findings show that the MnO_2 was uniformly coated on the ITO−PET, as evidenced by the semitransparent golden color of the material.[36] The MnO_2 was synthesized on the surface of the ITO−PET, by an electrodeposition method, as shown in Figure 2C. The morphology of the electrodeposited MnO_2 was observed to be vertically aligned with the shape of irregular nanoflower, as shown in Figure 2D. These structures are the result of the electrodeposition process,[37] and interconnected MnO_2 particles would be expected to improve electrolytic ion mobility.[38] The crystalline properties of synthesized MnO_2, which were grown on an ITO−PET substrate, were investigated for basal characterization, as shown in Figure S2A, SI. No obvious differences between the peaks for MnO_2/ITO−PET and ITO−PET were observed, which indicates that the synthesized MnO_2 has an amorphous structure, as previously reported,[39] due to the absence of a heat treatment process. Additional surface elemental analyses were performed with XPS to confirm the crystalline structure of the γ-MnO_2 (Figure S2B,C, SI).

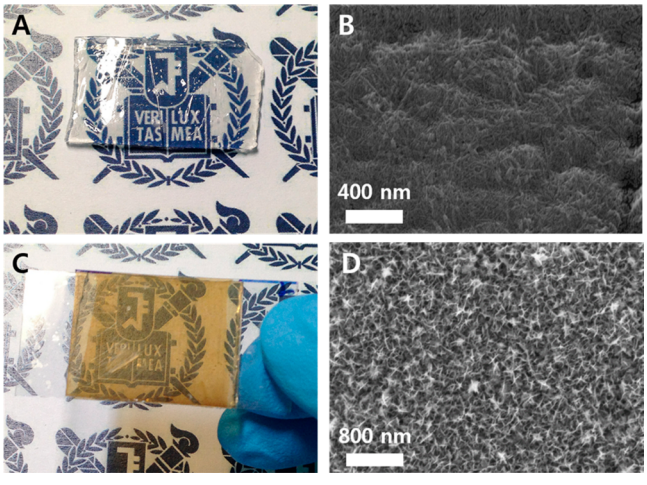

Figure 2. (A) Optical image and (B) SEM image of agarose gel. (C) Optical image and (D) SEM image of MnO_2 deposited ITO−PET.

The electrochemical properties and performance of a MnO_2/NaCl−AGAR/MnO_2 symmetric cell were evaluated by CV measurements using a potential window of 0−0.8 V as a function of different scan rates. To optimize the performance of the NaCl−AGAR, we studied CVs in different conditions at a scan rate of 20 mV s^{-1}. The dependency of CV performance on the thickness of the gel electrolyte was evaluated, and the results are shown in Figure S3A, SI. The CV curves were essentially the same among gels that were fabricated from 1 (0.5 mm), 2 (1.0 mm), and 3 (1.5 mm) blocks of overlapped glass plates, which indicates that the effects of electrolyte thickness on electrochemical performance are negligible.

For further investigation of electrical properties of NaCl−AGAR, specific capacitances, we obtained changes in phase angle and resistor-capacitor (RC) time constants as functions of frequency and thickness of NaCl−AGAR. Two Pt plates were introduced, and thereby the measurement was conducted with the feature of Pt/NaCl−AGAR/Pt symmetric cell assembly.[40]

As shown in Figure S4A (SI), the specific capacitances of different thicknesses of gel exhibited similar tendency as a function of frequency. Figure S4B (SI) also supports that the specific capacitances with respect to gel electrolyte thickness are not significantly changed in the frequency range of 1−1000 Hz. As shown in Figure S4C (SI), the phase angle for NaCl−AGAR at the range of frequencies below 100 Hz for 1, 2, and 3 block depth gels were measured to be around −80°, exhibiting capacitive responses.[40] A phase angle of −45° implies the transition between capacitive and resistive responses. All the depth featured phase angles of −45° around the frequency of 1 kHz and showed similar behaviors above the frequency of 100 Hz. Figure S4D (SI) reveals the RC polarization response times as a function of gel thickness. It was observed that the RC time constants were maintained consistently under the same frequency without influence of gel electrolyte thickness. Therefore, the effects of gel electrolyte thickness on electrochemical performance are negligibly low.

Hence, the minimum thickness in this experiment, 1 block gel electrolyte, was utilized as a criterion for the thickness for charge storage with high ion conductivity and for conferring the

DOI: 10.1021/am5070987
ACS Appl. Mater. Interfaces 2015, 7, 3503−3511

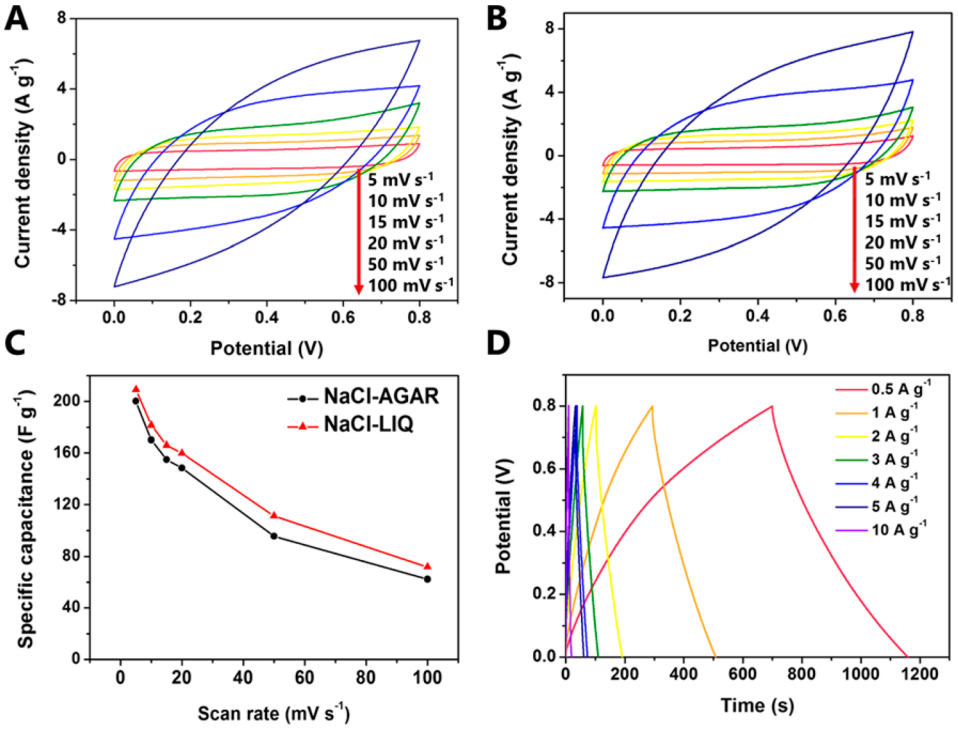

Figure 3. Rate dependent CVs for (A) NaCl–AGAR, (B) NaCl–LIQ over a range of 5–100 mV s^{-1}, and (C) normalized specific capacitance comparison of NaCl–AGAR and NaCl–LIQ at different scan rates. (D) Charge/discharge profile of NaCl–AGAR.

required flexibility. The shapes of all of the CV curves with NaCl concentrations from 0.1 to 0.5 M (Figure S3B, SI) were also essentially identical to one another. As the gross area of the substrate which is electrodeposited with MnO_2 is constant, the total amount of ions that can be inserted or removed on the surface of the electrode is assumed to be constant as well. Thus, it can be concluded that 0.1 M is an appropriate concentration for achieving full activation of the electrode. This concentration was used as the standard criterion for NaCl–AGAR. Figure S3C (SI) shows the CV profiles for varying deposition times for MnO_2 synthesis ranging from 100 to 300 s. The results show that a sample prepared using a deposition time of 200 s exhibited the highest current density among the samples tested. The relatively low quantity of sample electrodeposition for 100 s was not sufficient for achieving sufficient specific capacitances, and a condensed packing using a period of 300 s gives rise to a surface area of MnO_2 cannot be fully utilized.[41] Hence, the optimum time of 200 s was selected for MnO_2 electrodeposition time.

Figure 3A,B show the results of the CVs from the supercapacitors with the NaCl–AGAR and 0.1 M NaCl aqueous solution (NaCl–LIQ), respectively. For this comparison, a gel with a thickness of 0.5 mm (thickness of one glass plate) and NaCl concentration of 0.1 M were selected due to the negligible effects of gel thickness and NaCl concentration on electrochemical performance, on the basis of the above-mentioned criteria. CV curves for NaCl–AGAR and NaCl–LIQ showed quasi-rectangular and symmetrical shapes, indicating that the rate capability for NaCl–AGAR is comparable to that for NaCl–LIQ. In addition, similar shapes and current densities for CVs from both electrolytes as a function of scan rate suggest that the supercapacitive behavior of the NaCl–AGAR is unimpeded due to the excellent ion conductivity, which is comparable to the NaCl–LIQ. The specific capacitance calculated from the CVs for NaCl–LIQ was 209 F g^{-1}, which is slightly higher than that for NaCl–AGAR (200 F g^{-1}) at the lowest scan rate (5 mV s^{-1}). Moreover, the specific capacitance of the supercapacitor with NaCl–AGAR was 80% of that for the NaCl–LIQ at higher scan rates, 100 mV s^{-1}, which suggests that the performance of the NaCl–AGAR would be similar to that for NaCl–LIQ. The normalized specific capacitances of the symmetric supercapacitors for both NaCl–AGAR and NaCl–LIQ were plotted as a function of scan rates based on the specific capacitance of 5 mV s^{-1}, as shown in Figure 3C. It has been reported that the specific power of a supercapacitor is determined by how fast the ions are able to move.[42] In this regard, a supercapacitor with NaCl–AGAR showed a comparable rate capability to that for NaCl–LIQ. The decreases in specific capacitance with increasing scan rate for both electrolytes are due to the increase of charge resistance of the material.[43] Moreover, the similar degree of reduction for both electrolytes within the measured range of scan rates clarifies that the rate of ion mobility in the NaCl–AGAR is sufficiently fast to allow it to compete with NaCl–LIQ.[12] The charge and discharge behaviors of the supercapacitor with NaCl–AGAR was examined at current densities in the range of 0.5–10 A g^{-1} by using the same two-electrode system shown in Figure 3D. These galvanostatic curves exhibited triangular forms with a small internal resistance (IR) drop in a broad range of current densities, demonstrating excellent rate capability.[44] The specific capacitances for NaCl–AGAR, as estimated from the discharge time, were calculated to be 286.9 and 268.1 F g^{-1} at a current density of 0.5 and 1 A g^{-1}, respectively, which are similar to previously reported values for MnO_2 gel electrolyte based supercapacitors, as shown in Table S1 (SI).[38,45−47]

Electrochemical impedance measurements were performed in order to observe the resistivity behaviors of the super-

DOI: 10.1021/am5070987
ACS Appl. Mater. Interfaces 2015, 7, 3503−3511

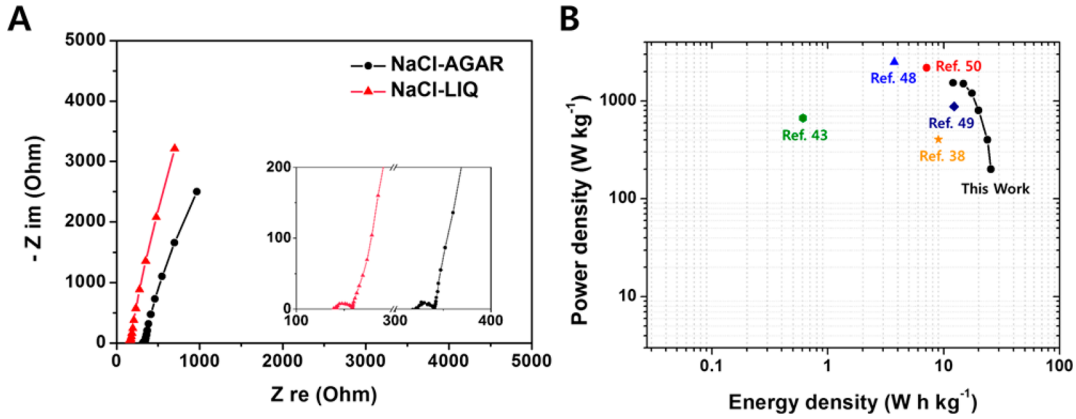

Figure 4. Comparison of (A) Nyquist impedance plot (B) Ragone plot of NaCl–AGAR and NaCl–LIQ.

capacitors fabricated by NaCl–AGAR and NaCl–LIQ, as shown in Figure 4A. The impedance results for NaCl–AGAR (318.1 Ω) showed a higher magnitude of ESR of the electrode material (an intercept on the real axis in the high frequency region) than that for NaCl–LIQ (139.1 Ω). This would be expected, since the charge transfer for NaCl–AGAR involves a relatively high contact resistance between the electrolyte and electrode than that for NaCl–LIQ caused by a liquid phase electrolyte based ion mobility. The contact loss may result in a reduction in specific capacitances, which is in good agreement with the relatively lower specific capacitances for NaCl–AGAR compared to that for NaCl–LIQ. The semicircular behavior at the high- to middle-frequency region which is related to the interfacial resistance between electrode material and electrolyte, showed matchable values (~20.9 Ω) under both electrolyte configurations. This is because the same redox reaction between electrolyte ions and the MnO_2 is involved in both electrolytes. It was also confirmed that the supercapacitors with both electrolytes are not involved in Warburg impedance, which represent the diffusivity of the electrolyte ions, based on the fact that there is no line that intersects the real axis near an angle of 45°.[9] The slope for the NaCl–LIQ sample is similar to that for the NaCl–AGAR sample, which is indicative of comparable power characteristic between the developed gel system and the conventional liquid system. The power characteristics can also be compared by a Ragone plot. Figure 4B shows the Ragone plot obtained from the total mass of active materials for both the positive and the negative electrodes. The result of Ragone plot for NaCl–AGAR showed a compatible performance compared with the recently reported MnO_2 based flexible supercapacitors.[38,43,48−50]

The excellent supercapacitive behavior of the NaCl–AGAR-based supercapacitor as a full cell can be attributed to the pore structure of NaCl–AGAR, which can provide various advantages for ion transport. According to the charge storage mechanism, MnO_2 can exhibit a Faradaic reaction in a sodium-based electrolyte system.[51] One of the effective parameters in determining the rate capability is the diffusivity and rate of insertion (or extraction) of participating protons and sodium ions in the redox reaction. Diffusivity can be enhanced by an intimate contact between the MnO_2 and electrolyte, as well as a low resistance to diffusion by composing an interconnected porous system, which could also promote the ionic adsorption of electrolyte ions onto the surface of the MnO_2. In this regard, NaCl–AGAR could effectively improve power density by providing compatible 3D channel networks filled with an electrolyte in an aqueous medium. We propose herein the schematic structure of NaCl–AGAR with the illustrative cross section of gel as shown in Figure 5. An agarose hydrogel

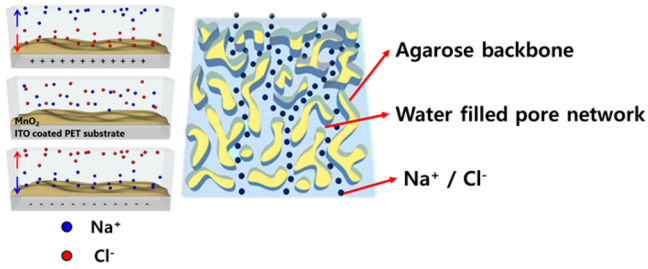

Figure 5. Proposed schematic design showing ion transport in the agarose gel.

consists of a 3D chemically interconnected agarose backbone and oriented interparticular submicropores filled with water, which is generated by a hydrogen-bonded cross-linking self-assembly mechanism. Positioned between the positive and negative electrodes, the gel electrolyte not only prevents the electrodes from coming into physical contact, but it also enables free ionic transport with a perfect isolation of electronic flow.[52] The functional enhancement of NaCl–AGAR can be ascribed to three factors. First, the skeleton of the agarose matrix confers excellent mechanical properties of the gel as a framework. The hydrogen bonding between the agarose polymers reinforce the formation of the 3D network and simultaneously improve mechanical stability. Second, the developed pores with the water filler provides an ion reservoir, thus providing an efficient ionic pathway to the storage sites of MnO_2.[53] Basically, ionic conductance can be easily improved within the agarose hydrogel by enveloping the aqueous ionic liquid.[29,54] Lowering the viscosity of the electrolyte by the introduction of a water filler facilitates the development of moist pore networks, which plays a significant role in ion conducting channels.[55] The accessibility of ions within the pore networks strongly depends on the sizes of the pores and the type of electrolyte ions.[53] The inner diameters of the pores in NaCl–AGAR, which are approximately on a submicrometer scale, would be sufficient to host the sodium and chloride ions. The fact that agarose gels are widely applied in DNA (bigger than Na^+ or Cl^-) electrophoresis supports this deduction.[56] Third, the addition of sodium chloride to agarose gel as electrolyte ions is also advantageous in terms of enhancing ionic

DOI: 10.1021/am5070987
ACS Appl. Mater. Interfaces 2015, 7, 3503−3511

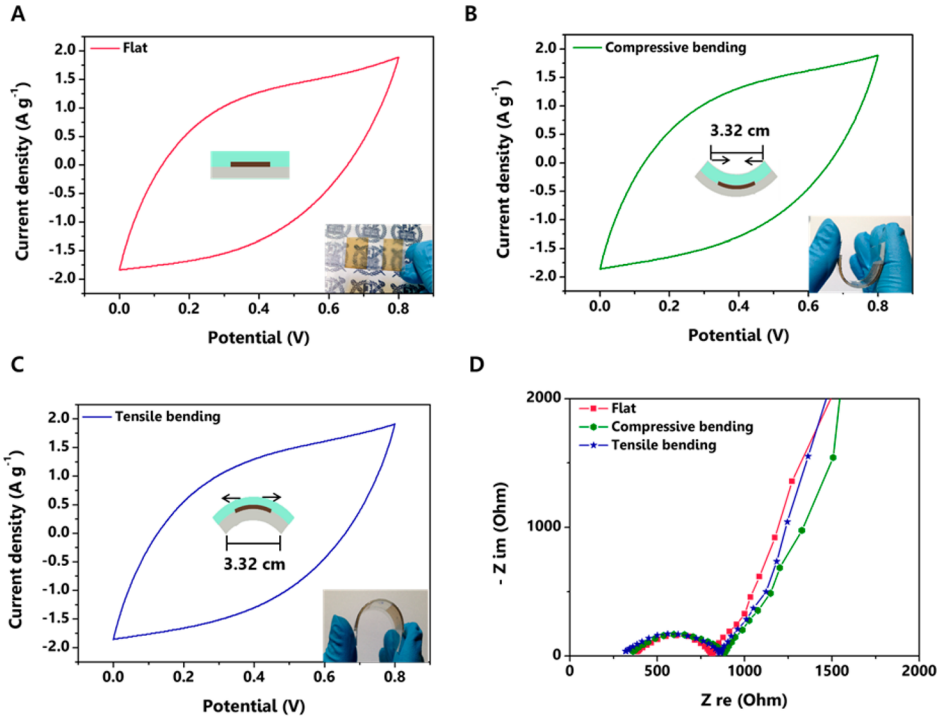

Figure 6. Comparing CV at a scan rate of 20 mV sec^{-1}, EIS profile of as-synthesized sample with digital photo of three different bending statuses: (A) flat, (B) compressive bending, (C) tensile bending. (D) EIS profile of the three bending statuses.

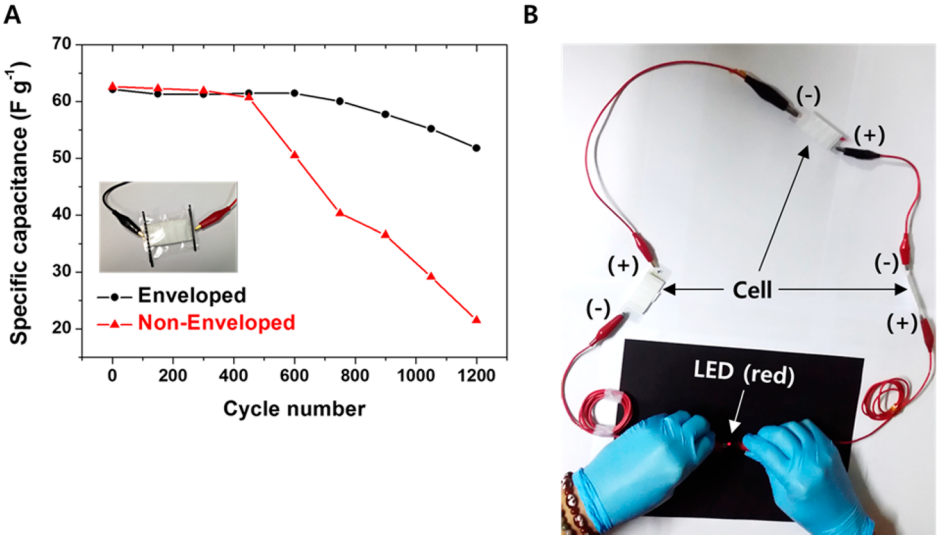

Figure 7. (A) Long cycle-term stability test profile of enveloped and nonenveloped NaCl−AGAR supercapacitors, performed at a scan rate of 100 mV sec^{-1} and (B) digital photo of an LED activated by the NaCl−AGAR supercapacitors.

conductivity. This is because Na^+ can inhibit electrode polarization, which can be caused by an increase in H^+ originating from the electrolysis of water molecules as the result of overcharging and overdischarging.[29] The ionic conductance of Na^+ can also be increased by the synergistic effect with negatively charged functionalities (sulfate, pyruvate, glucuronate, and others) on the agarose backbone.[29] Subsequently, the hierarchical pore structure of the NaCl−AGAR provide open spaces that facilitate the accessibility of electrolyte ions, resulting in an enhanced utilization of three-dimensionally located electrolyte ions within the pores.[26] Following this, an improved interfacial contact would provide electrochemical reciprocity for NaCl−AGAR.

To verify the flexible nature of the NaCl−AGAR, we designed a one-planar interdigitated prototype of supercapacitor. MnO_2 was electrodeposited on the same plane with a partition for arraying the cathode and anode in one planar configuration, which is depicted in Figure 6A−C insets. No significant deviation in the CV curves was observed when the NaCl−AGAR supercapacitor is bent with a bending radius of 1.16 cm; when it is flat (Figure 6A), as the result of compressive bending (in-plane conformation, Figure 6B), and of tensile bending (out-of-plane conformation, Figure 6C). We performed electrochemical impedance measurements to observe the resistive behaviors of the fabricated supercapacitor assembly under various bending conditions, as shown in Figure

DOI: 10.1021/am5070987
ACS Appl. Mater. Interfaces 2015, 7, 3503−3511

6D. Nyquist plots of three arrangements also feature almost equal semicircular behavior (~496.5 Ω), which suggests that comparable charge transfer rate under different bending status. These results indicate that the NaCl–AGAR is very stable under various bending conditions, and the resultant full-cell is suitable for flexible device applications.

We explored the stability of the NaCl–AGAR supercapacitors by CV at a scan rate of 100 mV s^{-1}. The variation in specific capacitances as a function of cycle number is shown in Figure 7A. The MnO_2/NaCl–AGAR/MnO_2 full cell during the retention test was thoroughly enveloped by PTFE sealant tape and sticky polypropylene tape, as shown in Figure 7A inset. The normalized specific capacitances (based on the specific capacitance at the 10th cycle) begin to decrease after 600 cycles and about 80% of the maximum capacity is retained after 1200 cycles. Compared with the 34% of capacity retention for the nonenveloped cell, the enveloped cell exhibited better cycle stability. The relatively superior durability for the enveloped sample which is consistent with previously reported data for MnO_2 cycle stability,[57,58] can be considerably ascribed to the retention of moist and interconnected ion transfer channels within the pore networks, caused by preventing the evaporation of water. This indicates that a NaCl–AGAR-based supercapacitor could exhibit a high stability with a substantial enhancement in enveloping process. Additionally, it was demonstrated that the assembled device can activate a red light emitting diode (Figure 7B).

Apparently, the most challenging issues in the state-of-the-art flexible energy storage systems are to maintain their original energy and power density. From the viewpoint of material design, there are various possible combinations of gel electrolytes and electrodes to improve these two key performances. Thus, we believe that the developed supercapacitor system with NaCl–AGAR has high potential to be further improved.

4. CONCLUSIONS

In summary, NaCl–AGAR was developed for use as a supercapacitor electrolyte material with enhanced electrochemical performance that matches that of a liquid electrolyte configuration. NaCl–AGAR has several advantages, in that it is simple, low-cost, and scalable and has a high capacitance performance. Owing to the 3D hierarchical porous network as an optimized ion transport channel in the gel, the fabricated gel electrolyte exhibits high specific capacitances and rate capability. In addition, the combination of NaCl and agarose gel ensures the safe fabrication and applications by means of gel electrolyte features with culinary, environmentally benign, biodegradable characteristics. Hence, we believe that NaCl–AGAR may offer attractive prospects and could be extended to further application because of its high performance, simplicity of fabrication, and eco-friendly properties.

■ ASSOCIATED CONTENT

Supporting Information

Details of calculations, XRD, XPS profiles, comparison of cyclic voltammetry results with variation of electrode condition, resistive study of NaCl–AGAR, and electrolyte configuration. This material is available free of charge via the Internet at http://pubs.acs.org.

■ AUTHOR INFORMATION

Corresponding Author

*E-mail: jyi@snu.ac.kr. Tel.: +82 2-880-7438.

Author Contributions

†These authors contributed equally to the work.

Notes

The authors declare no competing financial interest.

■ ACKNOWLEDGMENTS

This research was supported by the Global Frontier R&D Program on Center for Multiscale Energy System funded by the National Research Foundation under the Ministry of Science, ICT & Future, Korea (NRF-2011-0031571).

■ REFERENCES

(1) Winter, M.; Brodd, R. J. What Are Batteries, Fuel Cells, and Supercapacitors? *Chem. Rev.* **2004**, *104*, 4245–4269.

(2) Hall, P. J.; Mirzaeian, M.; Fletcher, S. I.; Sillars, F. B.; Rennie, A. J. R.; Shitta-Bey, G. O.; Wilson, G.; Cruden, A.; Carter, R. Energy Storage in Electrochemical Capacitors: Designing Functional Materials to Improve Performance. *Energy Environ. Sci.* **2010**, *3*, 1238–1251.

(3) Wang, G. P.; Zhang, L.; Zhang, J. J. A Review of Electrode Materials for Electrochemical Supercapacitors. *Chem. Soc. Rev.* **2012**, *41*, 797–828.

(4) Anothumakkool, B.; Torris, A. A. T.; Bhange, S. N.; Badiger, M. V.; Kurungot, S. Electrodeposited Polyethylenedioxythiophene with Infiltrated Gel Electrolyte Interface: A Close Contest of an All-Solid-State Supercapacitor with Its Liquid-State Counterpart. *Nanoscale* **2014**, *6*, 5944–5952.

(5) Li, L.; Wu, Z.; Yuan, S.; Zhang, X.-B. Advances and Challenges for Flexible Energy Storage and Conversion Devices and Systems. *Energy Environ. Sci.* **2014**, *7*, 2101–2122.

(6) Niu, Z.; Dong, H.; Zhu, B.; Li, J.; Hng, H. H.; Zhou, W.; Chen, X.; Xie, S. Highly Stretchable, Integrated Supercapacitors Based on Single-Walled Carbon Nanotube Films with Continuous Reticulate Architecture. *Adv. Mater.* **2013**, *25*, 1058–1064.

(7) Henderson, W. A.; Brooks, N. R.; Young, V. G., Jr. Single-Crystal Structures of Polymer Electrolytes. *J. Am. Chem. Soc.* **2003**, *125*, 12098–12099.

(8) Quartarone, E.; Mustarelli, P. Electrolytes for Solid-State Lithium Rechargeable Batteries: Recent Advances and Perspectives. *Chem. Soc. Rev.* **2011**, *40*, 2525–2540.

(9) Yang, X.; Zhang, F.; Zhang, L.; Zhang, T.; Huang, Y.; Chen, Y. A High-Performance Graphene Oxide-Doped Ion Gel as Gel Polymer Electrolyte for All-Solid-State Supercapacitor Applications. *Adv. Funct. Mater.* **2013**, *23*, 3353–3360.

(10) Croce, F.; Appetecchi, G. B.; Persi, L.; Scrosati, B. Nanocomposite Polymer Electrolytes for Lithium Batteries. *Nature* **1998**, *394*, 456–458.

(11) Kawasaki, M.; Iwasa, Y. Electronics: 'Cut and Stick' Ion Gels. *Nature* **2012**, *489*, 510–511.

(12) Lodge, T. P. A Unique Platform for Materials Design. *Science* **2008**, *321*, 50–51.

(13) Niu, Z.; Zhang, L.; Liu, L.; Zhu, B.; Dong, H.; Chen, X. All-Solid-State Flexible Ultrathin Micro-Supercapacitors Based on Graphene. *Adv. Mater.* **2013**, *25*, 4035–4042.

(14) Ding, X.; Zhao, Y.; Hu, C.; Hu, Y.; Dong, Z.; Chen, N.; Zhang, Z.; Qu, L. Spinning Fabrication of Graphene/Polypyrrole Composite Fibers for All-Solid-State, Flexible Fibriform Supercapacitors. *J. Mater. Chem. A* **2014**, *2*, 12355–12360.

(15) Wang, G.; Lu, X.; Ling, Y.; Zhai, T.; Wang, H.; Tong, Y.; Li, Y. LiCl/PVA Gel Electrolyte Stabilizes Vanadium Oxide Nanowire Electrodes for Pseudocapacitors. *ACS Nano* **2012**, *6*, 10296–10302.

(16) Huang, C.-W.; Wu, C.-A.; Hou, S.-S.; Kuo, P.-L.; Hsieh, C.-T.; Teng, H. Gel Electrolyte Derived from Poly(ethylene glycol) Blending Poly(acrylonitrile) Applicable to Roll-to-Roll Assembly of Electric Double Layer Capacitors. *Adv. Funct. Mater.* **2012**, *22*, 4677–4685.

DOI: 10.1021/am5070987
ACS Appl. Mater. Interfaces 2015, 7, 3503–3511

(17) Lee, J.; Panzer, M. J.; He, Y.; Lodge, T. P.; Frisbie, C. D. Ion Gel Gated Polymer Thin-Film Transistors. *J. Am. Chem. Soc.* **2007**, *129*, 4532−4533.
(18) Srinivasan, S.; Shin, W. H.; Choi, J. W.; Coskun, A. A Bifunctional Approach for the Preparation of Graphene and Ionic Liquid-Based Hybrid Gels. *J. Mater. Chem. A* **2013**, *1*, 43−48.
(19) Tako, M.; Nakamura, S. Gelation Mechanism of Agarose. *Carbohydr. Res.* **1988**, *180*, 277−284.
(20) Kim, G.-P.; Park, S.; Nam, I.; Park, J.; Yi, J. Preferential Growth of Co_3O_4 Anode Material with Improved Cyclic Stability for Lithium-Ion Batteries. *J. Mater. Chem. A* **2013**, *1*, 3872−3876.
(21) Ross, K. A.; Scanlon, M. G. Analysis of the Elastic Modulus of Agar Gel by Indentation. *J. Texture Stud.* **1999**, *30*, 17−27.
(22) Normand, V.; Lootens, D. L.; Amici, E.; Plucknett, K. P.; Aymard, P. New Insight into Agarose Gel Mechanical Properties. *Biomacromolecules* **2000**, *1*, 730−738.
(23) Duffus, C.; Camp, P. J.; Alexander, A. J. Spatial Control of Crystal Nucleation in Agarose Gel. *J. Am. Chem. Soc.* **2009**, *131*, 11676−11677.
(24) Clar, J. G.; Silvera Batista, C. A.; Youn, S.; Bonzongo, J. C.; Ziegler, K. J. Interactive Forces between Sodium Dodecyl Sulphate-Suspended Single-Walled Carbon Nanotubes and Agarose Gels. *J. Am. Chem. Soc.* **2013**, *135*, 17758−17767.
(25) Wang, X.; Egan, C. E.; Zhou, M.; Prince, K.; Mitchell, D. R. G.; Caruso, R. A. Effective Gel for Gold Nanoparticle Formation, Support, and Metal Oxide Templating. *Chem. Commun.* **2007**, 3060−3062.
(26) Koo, H.-J.; Chang, S. T.; Slocik, J. M.; Naik, R. R.; Velev, O. D. Aqueous Soft Matter Based Photovoltaic Devices. *J. Mater. Chem.* **2011**, *21*, 72−79.
(27) Singh, T.; Trivedi, T. J.; Kumar, A. Dissolution, Regeneration and Ion-Gel Formation of Agarose in Room-Temperature Ionic Liquids. *Green Chem.* **2010**, *12*, 1029−1035.
(28) Lu, S. Zn^{2+} Blocks Annealing of Complementary Single-Stranded DNA in a Sequence-Selective Manner. *Sci. Rep.* **2014**, *4*, 5464.
(29) Koo, H.-J.; Chang, S. T.; Velev, O. D. Ion-Current Diode with Aqueous Gel/SiO_2 Nanofilm Interfaces. *Small* **2010**, *6*, 1393−1397.
(30) Koo, H.-J.; So, J.-H.; Dickey, M. D.; Velev, O. D. Towards All-Soft Matter Circuits: Prototypes of Quasi-Liquid Devices with Memristor Characteristics. *Adv. Mater.* **2011**, *23*, 3559−3564.
(31) Cayre, O. J.; Chang, S. T.; Velev, O. D. Polyelectrolyte Diode: Nonlinear Current Response of a Junction between Aqueous Ionic Gels. *J. Am. Chem. Soc.* **2007**, *129*, 10801−10806.
(32) Mandal, L.; Deo, M.; Yengantiwar, A.; Banpurkar, A.; Jog, J.; Ogale, S. A Quasi-Liquid Iontronic−Electronic Light-Harvesting Hybrid Photodetector with Giant Response. *Adv. Mater.* **2012**, *24*, 3686−3691.
(33) Pernodet, N.; Maaloum, M.; Tinland, B. Pore Size of Agarose Gels by Atomic Force Microscopy. *Electrophoresis* **1997**, *18*, 55−58.
(34) Pluen, A.; Netti, P. A.; Jain, R. K.; Berk, D. A. Diffusion of Macromolecules in Agarose Gels: Comparison of Linear and Globular Configurations. *Biophys. J.* **1999**, *77*, 542−552.
(35) Maiti, U. N.; Lim, J.; Lee, K. E.; Lee, W. J.; Kim, S. O. Three-Dimensional Shape Engineered, Interfacial Gelation of Reduced Graphene Oxide for High Rate, Large Capacity Supercapacitors. *Adv. Mater.* **2014**, *26*, 615−619.
(36) Liu, D.; Zhang, Q.; Xiao, P.; Garcia, B. B.; Guo, Q.; Champion, R.; Cao, G. Hydrous Manganese Dioxide Nanowall Arrays Growth and Their Li^+ Ions Intercalation Electrochemical Properties. *Chem. Mater.* **2008**, *20*, 1376−1380.
(37) Chen, W.; Rakhi, R. B.; Hu, L.; Xie, X.; Cui, Y.; Alshareef, H. N. High-Performance Nanostructured Supercapacitors on a Sponge. *Nano Lett.* **2011**, *11*, 5165−5172.
(38) Nam, I.; Park, S.; Kim, G.-P.; Park, J.; Yi, J. Transparent and Ultra-Bendable All-Solid-State Supercapacitors without Percolation Problems. *Chem. Sci.* **2013**, *4*, 1663−1667.
(39) Xia, H.; Zhu, D.; Luo, Z.; Yu, Y.; Shi, X.; Yuan, G.; Xie, J. Hierarchically Structured Co_3O_4@Pt@MnO_2 Nanowire Arrays for High-Performance Supercapacitors. *Sci. Rep.* **2013**, *3*, 2978.
(40) Lee, K. H.; Zhang, S.; Lodge, T. P.; Frisbie, C. D. Electrical Impedance of Spin-Coatable Ion Gel Films. *J. Phys. Chem. B* **2011**, *115*, 3315−3321.
(41) Yu, Z.; Thomas, J. Energy Storing Electrical Cables: Integrating Energy Storage and Electrical Conduction. *Adv. Mater.* **2014**, *26*, 4279−4285.
(42) Korenblit, Y.; Rose, M.; Kockrick, E.; Borchardt, L.; Kvit, A.; Kaskel, S.; Yushin, G. High-Rate Electrochemical Capacitors Based on Ordered Mesoporous Silicon Carbide-Derived Carbon. *ACS Nano* **2010**, *4*, 1337−1344.
(43) Xu, Y.; Lin, Z.; Huang, X.; Liu, Y.; Huang, Y.; Duan, X. Flexible Solid-State Supercapacitors Based on Three-Dimensional Graphene Hydrogel Films. *ACS Nano* **2013**, *7*, 4042−4049.
(44) Yu, H.; Zhang, Q.; Joo, J. B.; Li, N.; Moon, G. D.; Tao, S.; Wang, L.; Yin, Y. Porous Tubular Carbon Nanorods with Excellent Electrochemical Properties. *J. Mater. Chem. A* **2013**, *1*, 12198−12205.
(45) Gao, Y.; Zhou, Y. S.; Qian, M.; Li, H. M.; Redepenning, J.; Fan, L. S.; He, X. N.; Xiong, W.; Huang, X.; Majhouri-Samani, M.; Jiang, L.; Lu, Y. F. High-Performance Flexible Solid-State Supercapacitors Based on MnO_2-Decorated Nanocarbon Electrodes. *RSC Adv.* **2013**, *3*, 20613−20618.
(46) Nam, H.-S.; Kwon, J. S.; Kim, K. M.; Ko, J. M.; Kim, J.-D. Supercapacitive Properties of a Nanowire-Structured MnO_2 Electrode in the Gel Electrolyte Containing Silica. *Electrochim. Acta* **2010**, *55*, 7443−7446.
(47) Peng, L.; Peng, X.; Liu, B.; Wu, C.; Xie, Y.; Yu, G. Ultrathin Two-Dimensional MnO_2/Graphene Hybrid Nanostructures for High-Performance, Flexible Planar Supercapacitors. *Nano Lett.* **2013**, *13*, 2151−2157.
(48) He, Y.; Chen, W.; Li, X.; Zhang, Z.; Fu, J.; Zhao, C.; Xie, E. Freestanding Three-Dimensional Graphene/MnO_2 Composite Networks as Ultralight and Flexible Supercapacitor Electrodes. *ACS Nano* **2013**, *7*, 174−182.
(49) Dai, S.; Xi, Y.; Hu, C.; Yue, X.; Cheng, L.; Wang, G. MnO_2@KCu_7S_4 NWs Hybrid Compositions for High-Power All-Solid-State Supercapacitor. *J. Power Sources* **2015**, *274*, 477−482.
(50) Meng, C.; Liu, C.; Chen, L.; Hu, C.; Fan, S. Highly Flexible and All-Solid-State Paperlike Polymer Supercapacitors. *Nano Lett.* **2010**, *10*, 4025−4031.
(51) Mai, L.; Li, H.; Zhao, Y.; Xu, L.; Xu, X.; Luo, Y.; Zhang, Z.; Ke, W.; Niu, C.; Zhang, Q. Fast Ionic Diffusion-Enabled Nanoflake Electrode by Spontaneous Electrochemical Pre-Intercalation for High-Performance Supercapacitor. *Sci. Rep.* **2013**, *3*, 1718.
(52) Hong, S. B.; Park, S. H.; Kim, J.-H.; Lee, S.-Y.; Kwon, Y. S.; Park, T.; Kang, P.-H.; Hong, S. C. Triple-Layer Structured Composite Separator Membranes with Dual Pore Structures and Improved Interfacial Contact for Sustainable Dye-Sensitized Solar Cells. *Adv. Energy Mater.* **2014**, *4*, 1400477.
(53) Zeller, M.; Lorrmann, V.; Reichenauer, G.; Wiener, M.; Pflaum, J. Relationship between Structural Properties and Electrochemical Characteristics of Monolithic Carbon Xerogel-Based Electrochemical Double-Layer Electrodes in Aqueous and Organic Electrolytes. *Adv. Energy Mater.* **2012**, *2*, 598−605.
(54) Trivedi, T. J.; Rao, K. S.; Kumar, A. Facile Preparation of Agarose−Chitosan Hybrid Materials and Nanocomposite Ionogels Using an Ionic Liquid via Dissolution, Regeneration and Sol−Gel Transition. *Green Chem.* **2014**, *16*, 320−330.
(55) Liu, X.; Wu, D.; Wang, H.; Wang, Q. Self-Recovering Tough Gel Electrolyte with Adjustable Supercapacitor Performance. *Adv. Mater.* **2014**, *26*, 4370−4375.
(56) Chu, H. S.; Choi, C. Y.; Won, J. I. Analysis and Comparison of Cloning Methods for the Preparation of Repetitive Polypeptides. *Korean J. Chem. Eng.* **2008**, *25*, 1125−1130.
(57) Chen, S.; Zhu, J.; Wu, X.; Han, Q.; Wang, X. Graphene Oxide-MnO_2 Nanocomposites for Supercapacitors. *ACS Nano* **2010**, *4*, 2822−2830.
(58) Zhang, Z.; Zhai, T.; Lu, X.; Yu, M.; Tong, Y.; Mai, K. Conductive Membranes of EVA Filled with Carbon Black and Carbon

DOI: 10.1021/am5070987
ACS Appl. Mater. Interfaces 2015, 7, 3503−3511

Nanotubes for Flexible Energy-Storage Devices. *J. Mater. Chem. A* **2013**, *1*, 505−509.

DOI: 10.1021/am5070987
ACS Appl. Mater. Interfaces 2015, 7, 3503−3511